

Mechanism of Morphological Transition from Lamellar/Perforated Layer to Gyroid Phases

Jong-Hyun Ahn and Wang-Cheol Zin*

Department of Materials Science & Engineering, Pohang University of Science and Technology, Pohang 790-784, Korea

Received Nov. 21, 2002; Revised Apr. 22, 2003

Abstract: We investigated epitaxial relations of phase transitions between the lamellar (L), hexagonally perforated layers (HPL), and gyroid (G) morphologies in styrene-isoprene diblock copolymer (PSI) and polyisoprene (PI)/PSI blend using rheology and small angle X-ray scattering (SAXS) techniques. In HPL→G transitions, six spot patterns of G phase were observed in two-dimensional SAXS pattern. On the other hand, in direct L→G transition without appearance of HPL phase, the polydomain patterns of G phase were observed. From present study, it was understood that direct L→G transition of blend may be suppressed by high-energy barrier of transition and mismatches in domain orientation between epitaxially related lattice planes.

Keywords: block copolymer, blend, SAXS, HPL, gyroid, phase transition, epitaxial relation.

Introduction

Block copolymers exhibit rich polymorphic behavior in melt, depending on the volume fraction of each block, f , and the product, χN , the interaction parameter and the number of the repeating units in the chain.¹ They self-assemble into a variety of periodic ordered microstructures such as lamellae (L), hexagonally ordered cylinder (HEX), body centered cubic (bcc).¹⁻⁵ Recent studies have found that the additional complex phases such as hexagonally perforated layers (HPL) and the gyroid (G) exist in the narrow region between L and HEX phases.³⁻⁶ HPL structure consists of alternating minority and majority component layers, in which hexagonally packed channels of majority component extend through the minority component. The HPL structure has also been known to be a long-lived non-equilibrium state that facilitates the transition from L to G phases. The G phase is formed from two distinct, interpenetrating networks of the minority component chains which are embedded in a matrix of majority component material.

The order-order phase transformation in block copolymer can occur epitaxially, where structural elements of the second phase grow from the first, without long-range transport of material, while preserving the orientation of some layer planes. However, the epitaxy between different ordered phases in block copolymer has been recently studied.^{7,8} In this work, we investigate the morphological changes and

epitaxial relations associated with L→G and HPL→G transitions in styrene-isoprene diblock copolymer.

Experimental

Materials. Styrene-isoprene diblock copolymer (PSI) and polyisoprene (PI) were synthesized by living anionic polymerization using high vacuum techniques. The characteristics of the samples are given in Table I. The polymer was dissolved in toluene as 10 wt% in the presence of 0.5 wt% anti-oxidant (Irganox 1010, Ciba-Geigy Group). The solution was cast at room temperature for 1 week and then dried in a vacuum oven at 100 °C for 36 hrs. After complete removal of the solvent, the samples were annealed under vacuum at 120 °C for 24 hrs before the measurement. To observe morphological transitions, the weight fraction of homopolymer PI in the blend was designed to be 2.5 wt% (The total volume fraction of isoprene in the blend = 0.35).

Rheological Measurements. Using an advanced rheometric expansion system (ARES) with parallel plates of

Table I. Characteristics of Polymers Used

Sample Code	M_w^a	M_w/M_n^b	f_{PI} (wt%) ^c	Unsaturation of PI (wt%) ^c	
				<i>cis</i> 1,4	<i>trans</i> 1,4
PSI	34000	1.02	30	68.3	26.4
PI	7000	1.05	100	65.3	28.2

^aby low-angle laser light scattering (LALLS).

^bby GPC calibrated with PS standard. ^cby ¹H-NMR.

*e-mail : wczin@postech.ac.kr

1598-5032/06/152-05 © 2003 Polymer Society of Korea

25 mm in diameter, dynamic temperature sweep experiments were performed under a nitrogen environment with temperatures decreasing or increasing at a rate of 1 °C/min. The frequency (ω) of 0.1 rad/s and the strain amplitude (γ) of 0.1% were applied to the sample during heating and cooling. Alignment of sample was achieved by a large amplitude oscillatory shear. A frequency of 0.1 rad/s with 100% strain amplitude was applied at 140 °C for 2 hrs. This process was efficient to remove the grain boundary between microdomains in the samples.

Small-angle X-ray Scattering (SAXS). SAXS measurements were performed at 1B2 beamline using synchrotron X-ray radiation sources at Pohang Accelerator Laboratory, Korea. The wavelength of X-ray source was 1.377 Å. The correction for smearing effect by the finite cross section of the incident beam was not necessary for the optics of SAXS with point focusing (0.2 × 0.2 mm). Samples were placed into a sample holder of hot-stage controlled by a set of thermoelectric devices. Two-dimensional (2-D) diffraction patterns were recorded on imaging plates and 2-D CCD camera. The distance between sample and imaging plate was 1.2 m. The intensity of scattering was measured over a range of scattering vectors, q , which for elastic scattering can be defined

$$q = 4\pi \sin \theta / \lambda \quad (1)$$

where θ is the scattering angle and λ is the wavelength of the incident beam.

Two orientations were studied. We designate x as the flow direction, y as the velocity gradient direction, and z as the vorticity direction as shown in Figure 1. To study orientation normal to the x direction, a strip of 1 mm thick in the flow direction was cut and X-rays were passed through the

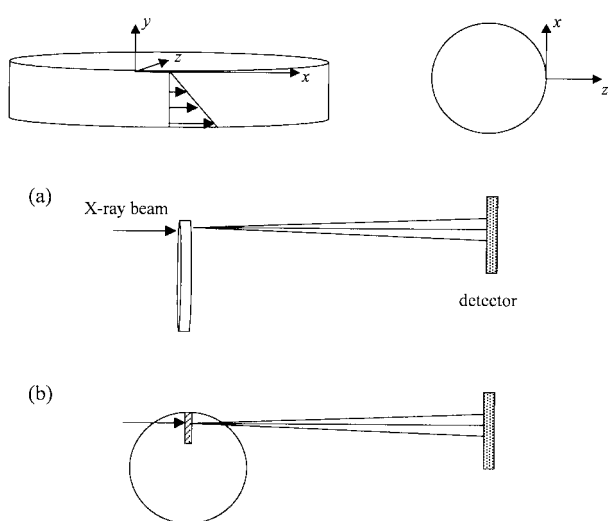


Figure 1. Definition of the axis system for the shear experiments. (a) parallel alignment and (b) perpendicular alignment.

slice as shown in Figure 1(a). A 1 mm slice was made near the edge of the sample disk in order to study orientation normal to the y direction. Figure 1(b) shows how X-rays pass through the sample in this case. Diffraction peaks indicate either parallel or perpendicular alignment, depending on their orientation.

Results and Discussion

Figure 2 shows elastic modulus (G') for PSI and PSI/PI blend at a rate of 1 °C/min, a frequency of 0.1 rad/s and a 1% strain amplitude. The values of G' for PSI continuously decrease with increasing temperature until 160 °C, at which they start to increase suddenly, indicating a phase transition between two ordered states (Figure 2(a)). Also, the PSI/PI blend begins to transform at 185 °C from low temperature morphology to high temperature one (Figure 2(b)).

Figure 3(a) shows SAXS profiles ($\log I(q)$ vs q) measured at room temperature for PSI. Three peaks spaced at approximate position ratios of 1 : 2 : 3 were observed, which is similar to the case of L morphology. However, the peaks are somewhat asymmetry, indicating the microstructure is not simple L phase (This morphology will be explained in detail below). The SAXS profile obtained at 180 °C on heating is shown in Figure 3(b). Two strong peaks observed in the ratio of $6^{1/2} : 8^{1/2}$ and high position peaks are consistent with

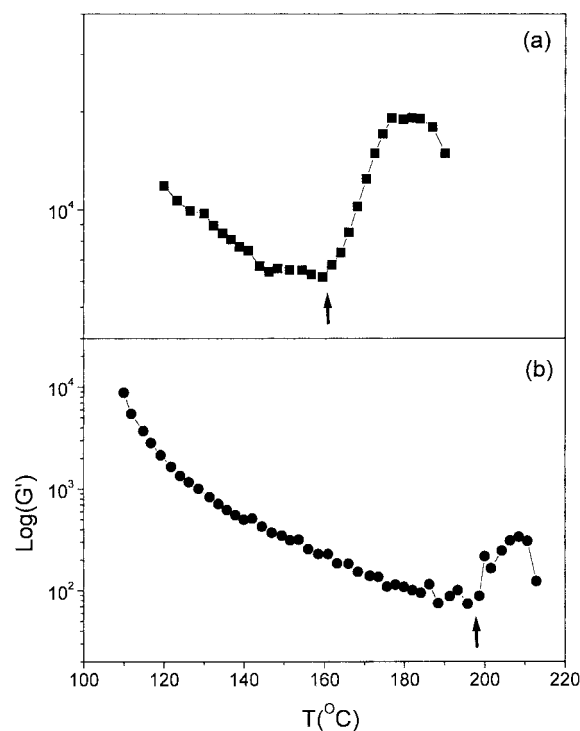


Figure 2. Temperature dependence of dynamic shear moduli for PSI (a) and PSI/PI blend (b) at shearing conditions of $\omega = 0.1$ rad/s, $\gamma = 1\%$ and heating/cooling rate = 1 °C/min.

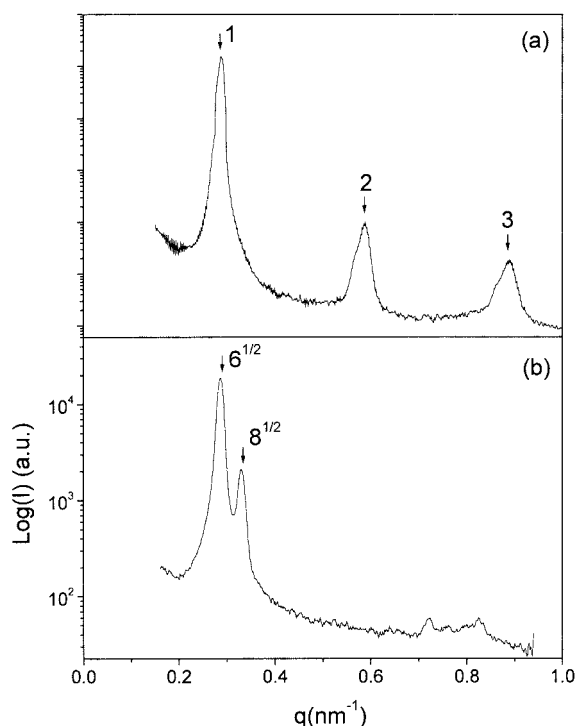


Figure 3. SAXS patterns of PSI. (a) a layered like morphology at 25 °C with asymmetry reflections in position ratio of 1 : 2 : 3 and (b) Gyroid phase with reflections in position ratio of $6^{1/2}$: $8^{1/2}$.

a G phase. These scattering profiles indicate a transition from a layered like morphology to G phase. Figure 4(a) shows SAXS profiles measured at room temperature for PSI/PI blend. In contrast to SAXS pattern of PSI, the pattern of blend shows symmetrical three peaks at relative position ratios of 1 : 2 : 3. It suggests that the blend is a L phase. On heating the sample to 180 °C, a morphological transition was not observed though it was annealed for 30 min. After subsequently heating the sample to 200 °C, the SAXS profile shows two peaks at relative ratio of $6^{1/2}$: $8^{1/2}$ as shown by the arrow, indicative of a G phase (Figure 4(b)). These scattering profiles and rheological data support that the blend transforms from L morphology to G phase.

Synchrotron SAXS experiments were performed with 2-D detector system in order to analyze the symmetries of HPL and G structure producing the off-axial scattering. These SAXS patterns are shown in Figures 5 and 6. Figure 5(a) shows the SAXS pattern of PSI at 140 °C, which indicates the long-range single-crystal-like orientation. The strong meridional reflections at ratios of 1 : 2 relative to the position of the first order maximum (q^*) in the q_y - q_z plane reveal that layer planes are aligned in parallel with the shear planes. In addition to the four off-meridional reflections in the inner lowest reflections (at $68 \pm 1^\circ$ with respect to the meridian and at $q = 0.91q^*$), the four off-meridional reflections (at $53 \pm 1^\circ$ with respect to the meridian and at $q = 1.06q^*$) char-

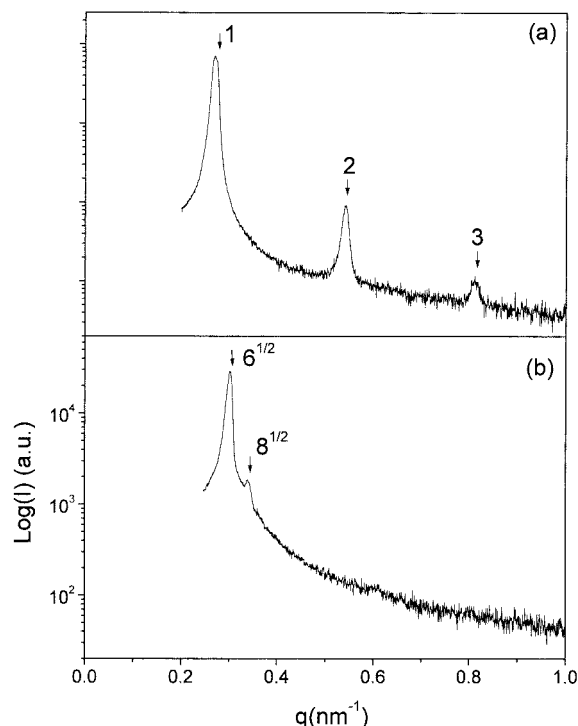


Figure 4. SAXS patterns of PSI/PI blend. (a) Lamellar morphology at 25 °C with symmetry reflections in position ratio of 1 : 2 : 3 and (b) Gyroid phase with reflections in position ratio of $6^{1/2}$: $8^{1/2}$.

acterize the stacking of the in-plane perforations. It means that the microstructure of PSI is not L but HPL phase.⁶ The scattering patterns corresponding to those of G phase appear on heating the sample to 180 °C. Figure 5(b) shows the contour plots of SAXS pattern at this temperature. Two sets of Bragg peaks with six-fold symmetry are observed in the ratio of $6^{1/2}$: $8^{1/2}$. The lowest order reflections correspond to the family of first order {211} reflections in G phase. Two of them are on the same parallel line as the strong meridional peaks from the layers in HPL structure. This result confirms the previous findings^{4,8} for an epitaxial relationship between {211} planes of G phase and the layer of HPL. Higher order reflections are also seen in scattering pattern. In q_y - q_z plane, {220} diffraction peaks are located at $\pm 30^\circ$ relative to the first order {211} reflections. These two sets of six-spot pattern duplicate the previous SANS data obtained when G phase has been grown from the shear-aligned hexagonally packed cylinder phase.⁷ Figure 5(c) shows the SAXS patterns obtained after cooling from 180 to 140 °C. These SAXS patterns indicate only the characteristic reflections of the G phase without showing the indication of a partial transformation to the HPL structure. This indicates that the HPL structure is unusually long-lived nonequilibrium structure.

On the other hand, the SAXS pattern of PSI/PI blend at 140 °C shows only two clear peaks at ratio of 1 : 2 relative to the position of the first order maximum without any off-

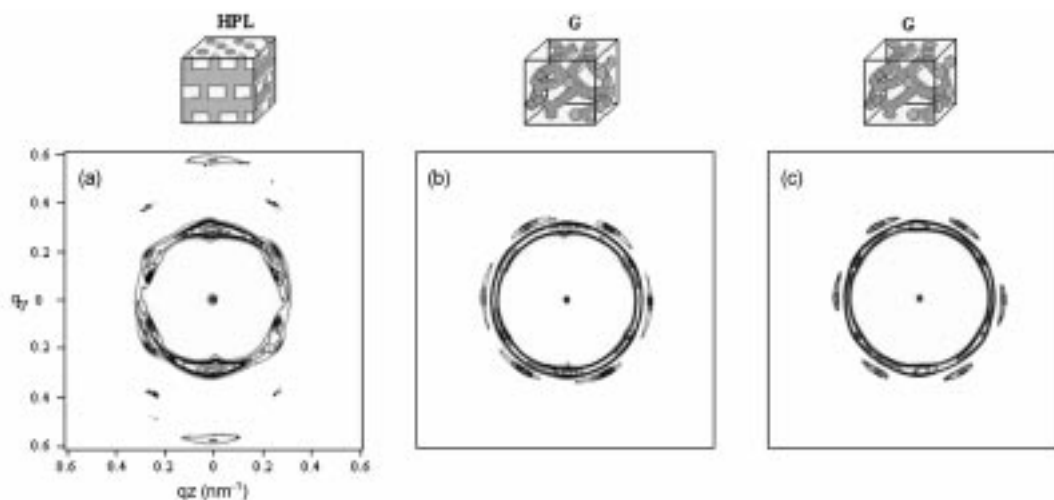


Figure 5. Contour plots of SAXS patterns obtained from the shear-oriented PSI at different temperature. (a) SAXS pattern at 25 °C. The diffraction pattern shows {101}, {003}, {102}, {104}, {105}, and {006} reflections of shear-oriented HPL structure,⁶ (b) After heating to 180 °C, SAXS pattern shows six {211} and six {220} reflections with 6-fold symmetry of the G phase, and (c) After cooling from 180 °C to 140 °C.

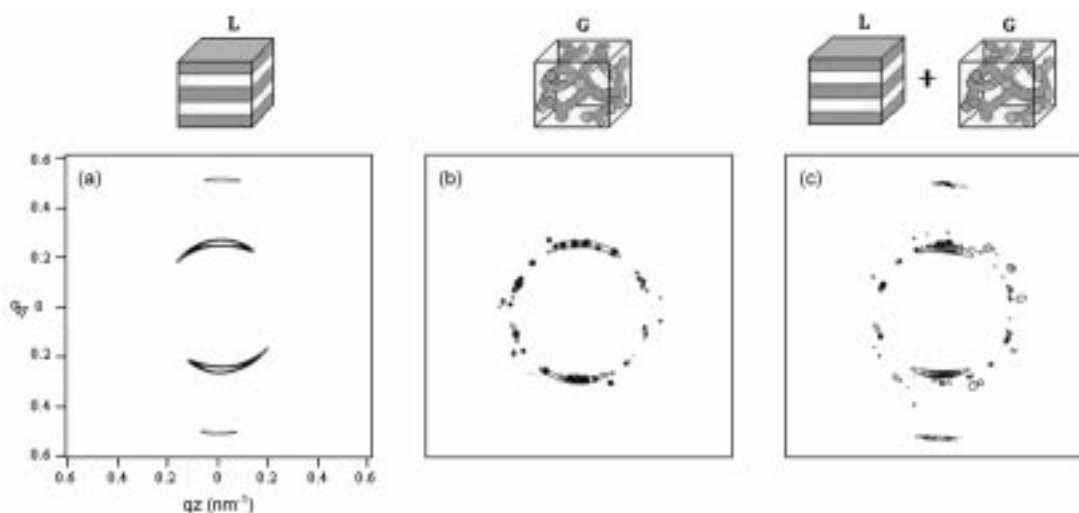


Figure 6. Contour plots of SAXS patterns obtained from the shear-oriented PSI/PI blend at different temperature. (a) The pattern of shear-oriented L structure at 140 °C, (b) After heating to 200 °C, the L structure transforms to the G phase, and (c) After cooling from 200 °C to 140 °C.

meridional reflections, which indicates not HPL phase but L phase. On heating the sample to 180 °C, the scattering pattern does not show any distinct change after annealing for 30 min. After heating the sample to 200 °C, the characteristic of G phase then begins to appear (Figure 6(b)). In contrast to the SAXS pattern of PSI, the pattern of PSI/PI blend shows the formation of polydomain, and it can be indexed as reflections from {211} and {220} planes of the G lattice. The presence of these reflections suggests that the G phase of the blend does not constitute a directionally oriented single-domain but a polydomain. Figure 6(c) shows the

SAXS pattern obtained after cooling the G morphology to 140 °C at which L was initially observed. The SAXS pattern indicates the coexistence of L and G phases. It reflects slow kinetic G→L transition due to a strain-dependent contribution to surface energy. Here, it is worthwhile to note that the SAXS pattern observed in L→G transition is different from that in HPL→G transition. The morphological transition from L phase to G phase proceeds through nucleation and growth and the difference in the geometrical characteristics of two phases induces considerable local distortion of both morphologies during transition.⁹ The resulting strain raises the

surface energy of the grains. The L→G transition is suppressed by this effect. Therefore, HPL phase tends to appear as an intermediate structure capable of forming low-energy grain boundaries during L→G transition. The HPL→G transition can proceed with epitaxial relation via nucleation and growth because both HPL and G morphologies are constructed from nearly-identical, 3-fold-coordinated minority component. However, PSI/PI blend shows direct L→G transitions without appearance of the HPL phase. It may be understood by both composition effects and a packing frustration. Hajduk *et al.* reported that in the block copolymer system, transition kinetics depend on the system composition.¹⁰ In PSI/PI blend, the L microdomain is more favorable than the HPL phase since the volume fraction of PI block component and symmetry of microdomain is increased by the addition of PI homopolymer to PI block. For an asymmetric block copolymer like the present case, the packing frustration can also play an important role in the morphological stability. Packing frustration has been reported for asymmetric copolymer with curved interface and described as a tendency to form domains of uniform thickness so that none of the constituent molecules are excessively stretched.^{11,12} In the HPL phase, a packing frustration is induced by the hexagonally packed channels formed by major component material through the minor component layer. In our previous work,¹³ we found that the addition of low molecular weight homopolymer to a minor component of HPL phase could reduce the packing frustration imposed on copolymers, and the effect could stabilize the HPL phase. On the other hand, addition of relatively high molecular weight homopolymer to copolymer cannot effectively fill the corners of Wigner-Seitz cells and cannot relieve some of the packing frustration, and the HPL phase cannot be stabilized. In PSI/PI blend, the HPL phase may not be formed as an intermediate structure, because relatively high molecular weight PI added to copolymer (the molecular weight ratio of PI to PI block = 0.69) cannot sufficiently reduce the stress by the packing frustration. Therefore, because of high-energy barrier of transition and mismatches in domain orientation between epitaxially related lattice planes, direct L→G transition of blend has

much difficulty in proceeding with an epitaxial relation. As a result, the sample nucleates multiple G phase grains with various orientations.

In summary, in this study we found that there is a clear dissimilarity of epitaxy between HPL→G and L→G transitions. HPL morphology transforms to G phase epitaxially and directly due to low-energy barrier. On the other hand, direct L→G transition of blend may have much difficulty in proceeding with an epitaxial relation due to high-energy barrier and mismatches in domain orientation.

Acknowledgements. This work was supported by the Center for Advanced Functional Polymers. The assistance of the Pohang Accelerator Laboratory in performing in SAXS measurements is gratefully acknowledged.

References

- (1) L. Leibler, *Macromolecules*, **13**, 1602 (1980).
- (2) M. J. Park, K. Char, H. D. Kim, C. H. Lee, B. S. Seong, and Y. S. Han, *Macromol. Res.*, **10**, 325 (2002).
- (3) D. A. Hajduk, P. E. Harper, S. M. Gruner, C. C. Kim, and E. L. Thomas, and L. J. Fetters, *Macromolecules*, **27**, 4063 (1994).
- (4) S. Förster, A. K. Khandpur, J. Zhao, F. S. Bates, I. W. Hamley, A. J. Ryan, and W. Bras, *Macromolecules*, **27**, 6922 (1994).
- (5) A. K. Khandpur, S. Förster, F. S. Bates, J. Zhao, A. J. Ryan, W. Bras, and I. W. Hamley, *Macromolecules*, **28**, 8796 (1995).
- (6) J.-H. Ahn and W.-C. Zin, *Macromolecules*, **33**, 641 (2000).
- (7) M. F. Shulz, F. S. Bates, K. Almdal, and K. Mortensen, *Phys. Rev. Lett.*, **73**, 86 (1994).
- (8) M. E. Vigild, K. Almdal, K. Mortensen, I. W. Hamley, J. P. A. Faiclough, and A. J. Ryan, *Macromolecules*, **31**, 5702 (1998).
- (9) D. A. Hajduk, R.-M. Ho, M. A. Hillmyer, F. S. Bates, and K. Almdal, *J. Phys. Chem. B*, **102**, 1356 (1998).
- (10) D. A. Hajduk, H. Takenouchi, M. A. Hillmyer, and F. S. Bates, *Macromolecules*, **30**, 3788 (1997).
- (11) D. C. Turner and S. M. Gruner, *Biochemistry*, **31**, 1340 (1992).
- (12) F. S. Bates and M. W. Matsen, *Macromolecules*, **29**, 7641 (1996).
- (13) J.-H. Ahn and W.-C. Zin, *Macromolecules*, **35**, 10238 (2002).